Adsorption geometry of carboxylic acid functionalized porphyrin molecules on TiO2(110)

Cynthia C. Fernández[a], Daniel Wechsler[b], Tulio C.R. Rocha[c], Hans-Peter Steinrück[b], Ole Lytken[b,*], Federico J. Williams[a,b,*]

[a] Departamento de Química Inorgánica, Analítica y Química Física, Facultad de Ciencias Exactas y Naturales, INQUIMAE-CONICET, Universidad de Buenos Aires, Ciudad Universitaria, Pabellón 2, Buenos Aires C1428EHA, Argentina
[b] Lehrstuhl für Physikalische Chemie II, Universität Erlangen-Nürnberg, Egerlandstraße 3, Erlangen 91058, Germany
[c] Brazilian Synchrotron Light Laboratory (LNLS), Brazilian Center for Research on Energy and Materials (CNPEM), Campinas 13083-970, Brazil

ABSTRACT

Controlling the adsorption geometry of porphyrin molecules on titania surfaces is an important step in the rational design of molecular devices such as dye-sensitized solar cells. We employed X-ray Photoelectron Spectroscopy (XPS) and Near-Edge X-Ray-Absorption Fine Structure (NEXAFS) spectroscopy to determine the binding mode, the electronic structure and the adsorption geometry of carboxylic acid functionalized tetra-phenylporphyrin molecules. Molecules with one (*mono*), two (*cis* and *trans*) and four (*tetra*) carboxylic acid anchoring groups were adsorbed on rutile TiO2(110). XPS shows that the iminic nitrogen atoms at the macro-cycle center are partially protonated after adsorption, and that the degree of protonation increases with the number of –COOH functional groups in the molecule. NEXAFS measurements show that molecules with either one or two groups in *cis* configuration adsorb with the macrocycle tilted away from the surface. In contrast, molecules with two carboxylic-acid groups in *trans* configuration adsorb with what is probably a flat-lying, but distorted macrocycle. Finally, molecules with four carboxylic-acid groups show no linear dichroism, indicating an intermediate adsorption angle. Our results show how the number and position of the –COOH functional groups determine the molecular adsorption geometry.

1. Introduction

The design of functional interfaces and nanoscale molecular architectures involves the attachment of complex molecular structures to solid surfaces [1]. Porphyrins are ideal for the functionalization of surfaces as they provide a robust molecular framework with strong absorption in the visible region and good photostability. Furthermore, changing functional groups or metal centers allows for tuning their electronic structure, optical and magnetic properties, chemical reactivity and employing anchoring groups for surface attachment [2]. Thus, porphyrins are key components in molecular materials with unique electronic, magnetic and photophysical properties [3], including chemical sensors [4], molecular catalysts [5], organic light-emitting devices [6] and dye sensitized solar cells [7]. This latter application is particularly important as it provides a flexible technology for low cost generation of renewable energy with reasonable efficiency [8].

Dye-sensitized solar cells involve the attachment of typically carboxylic acid functionalized porphyrins to TiO2 surfaces. The overall performance of the device depends on the details of the semiconductor/organic molecule interface. Therefore, fundamental studies on the interaction of porphyrins with TiO2 surfaces are of great importance. Consequently, there have been considerable recent efforts to study the adsorption of carboxylic acid functionalized porphyrins on TiO2 single crystal surfaces. Tetraphenylporphyrin (without carboxylic-acid anchoring groups) adsorbs on TiO2(110) at room temperature in a flat-lying geometry with partial protonation of the iminic nitrogen atoms [9,10]. Heating to 400 K results in self-metalation of the porphyrin molecules after incorporation of a titanyl group at the macrocycle center [9,11]. Functionalization of tetraphenylporphyrin with one carboxylic acid group results in covalent attachment of the molecule and formation of a carboxylate bond with the TiO2(110) surface [12]. Furthermore, at monolayer coverages carboxylic acid-functionalized tetraphenylporphyrin molecules adsorb with the macrocycle tilted away from the surface on TiO2 and Co3O4(111) [13,14]. Adding two
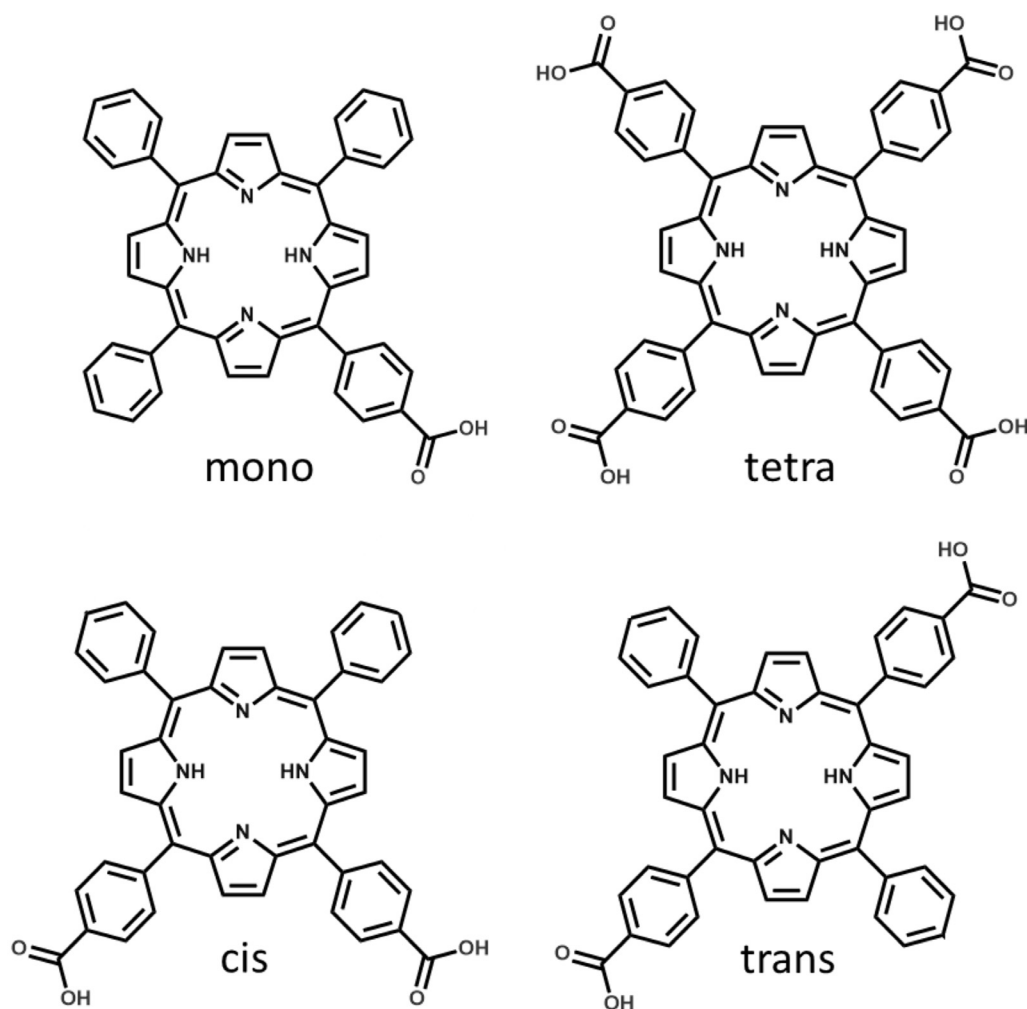
Fig. 1. Molecular structure of the *mono*, di (*cis* and *trans*) and *tetra* carboxylic acid-functionalized tetraphenylporphyrins. *mono*: 5-mono(4-carboxyphenyl)-10,15,20-(triphenyl) porphyrin, *tetra*: meso-tetra(4-carboxyphenyl) porphyrin, *cis*: 5,10-di-(4-carboxyphenyl) − 15,20-(diphenyl) porphyrin, *trans*: 5,15-(di-4-carboxyphenyl) − 10,20-(diphenyl) porphyrin.

functional groups in a *cis* configuration to Zn porphyrins results in a tilted monolayer [15]. On the other hand, Zn tetraphenylporphyrin with two carboxylic acid functional groups in a *trans* configuration results in flat-lying molecules [16]. Finally, Cu tetraphenylporphyrin with four functional groups also adsorbs in a flat-lying geometry at low coverages [17]. In most of these investigations, the porphyrins are deposited by thermal evaporation in vacuum.

In this work, we studied the molecular and electronic structure of *mono-, cis-, trans-* and *tetra*-functionalized tetraphenylporphyrin (see Fig. 1) adsorbed on TiO$_2$(110) surfaces at the solid/liquid interface. We employed X-ray photoelectron spectroscopy (XPS) and Near-Edge X-Ray-Absorption Fine Structure (NEXAFS) measurements to determine the binding mode, the adsorbate electronic structure, and the tilt angle of the macrocycle ring. Our results show that the number and position of carboxylic acid functional groups play an important role in the molecular structure of porphyrins deposited at the solid/liquid interface on oxide surfaces.

2. Experimental methods

All studies were carried out using a rutile TiO$_2$(110) single crystal (CrysTec GmbH). Carboxylic acid-functionalized porphyrins were obtained from Porphyrin-Laboratories (5-mono(4-carboxyphenyl)-10,15,20-(triphenyl) porphyrin and 5,10-di-(4-carboxyphenyl)-15,20-(diphenyl) porphyrin), PorphyChem (5,15-(di-4-carboxyphenyl)-10,20-

(diphenyl) porphyrin) and TriPorTech GmbH (meso-tetra(4-carboxyphenyl) porphyrin) and used as received. Absolute ethanol of analytical grade was used to prepare solutions. The TiO$_2$(110) sample was cleaned in UHV by several sputtering and annealing cycles. This resulted in XP spectra showing only substrate-related peaks and the expected TiO$_2$(110)-(1 × 1) LEED pattern [12]. The clean crystal was transferred outside UHV and immediately immersed in a 0.1 mM porphyrin solution in ethanol for 1 min. After removal from the solution, the sample was rinsed vigorously in a 25 ml stream of ethanol from a syringe, dried using an argon jet and transferred back into UHV for measurement. Although evaporation in vacuum is usually used to deposit porphyrin molecules here we could not use it as heating in vacuum resulted in decomposition of some of the molecules studied.

The synchrotron XPS and NEXAFS measurements were carried out at the Brazilian Synchrotron Light Source (LNLS) using the Planar Grating Monochromator (PGM) beamline for soft X-ray spectroscopy (100–1500 eV). Experiments were carried out at the Photoemission End Station with a base pressure of 2 × 10^{-10} mbar. NEXAFS spectra were obtained by measuring total electron yield (electron current from sample to ground), corrected for photon flux (electron current from a Au mesh to ground) measured simultaneously, and normalized to the edge jump. Porphyrin coverages are based on the N 1s to Ti 2p ratios, using as reference the 2HTPP monolayer on TiO$_2$(110) left behind after multilayer desorption [9]. Thus, one monolayer corresponds to the amount of nitrogen equivalent to a flat-lying layer of 2HTPP on
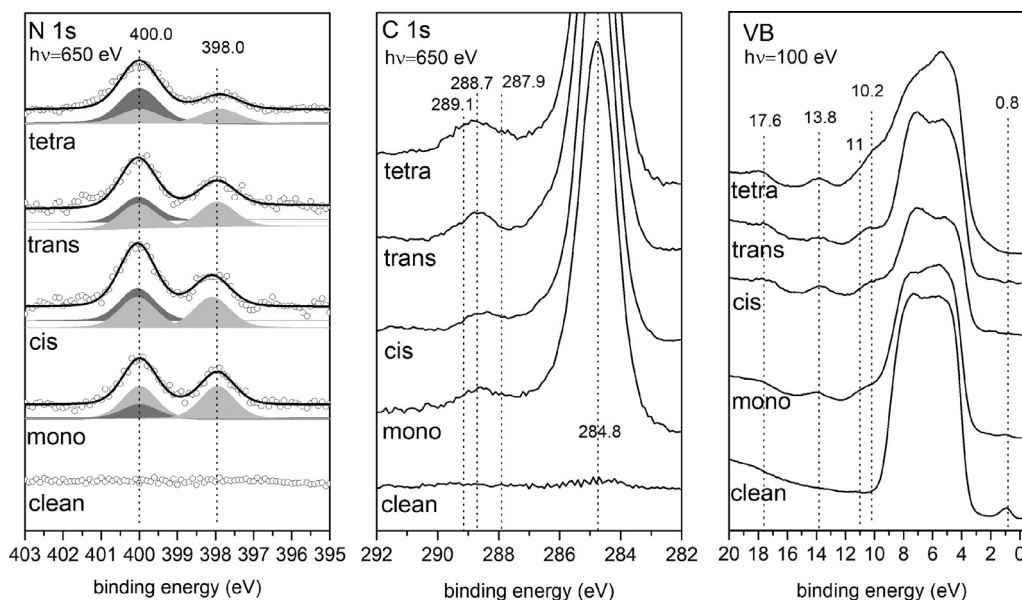
Fig. 2. N 1s, C 1s and valence-band XPS spectra of the clean TiO$_2$(110) substrate and after the adsorption of *mono, cis, trans* and *tetra* carboxylic-acid-functionalized tetraphenylporphyrin molecules.

TiO$_2$(110).

3. Results and discussion

We studied the adsorption of tetraphenylporphyrins containing one, two (in a *cis* and *trans* configuration) and four carboxylic acid functional groups on TiO$_2$(110). Fig. 1 shows the structure of the molecules studied. For simplicity, we refer to the tetraphenylporphyrin with one functional group as *mono*, with two functional groups as either *cis* or *trans*, depending on the configurational isomerism, and with four functional groups as *tetra*.

Fig. 2 displays the N 1s, C 1s and valence band XPS spectra corresponding to the clean TiO$_2$(110) substrate and to 1.1 ML of *mono*, 1.3 ML of *cis*, 1.0 ML of *trans* and 1.0 ML of *tetra* tetraphenylporphyrin. The N 1s spectra shows two signals at 398.0 and 400.0 eV, corresponding to the iminic and aminic nitrogen atoms, respectively [18]. In principle, the iminic-to-aminic intensity ratio should be 1:1 as shown by the light color-filled curves. However, in order to obtain a successful fit for the spectra in Fig. 2 a new dark color filled peak should be added at approximately 400 eV. This results in an iminic-to-aminic ratio of 1:1.4 for *mono*, 1:2 for *cis*, 1:2 for *trans*, and 1:3.4 for *tetra* porphyrins. This behavior has been previously ascribed to a protonation of the iminic nitrogen atoms which gives a peak at around 400 eV [9,10,12]. For vacuum-deposited molecules the protons could be supplied by the deprotonation of the carboxylic-acid groups or by hydroxyl groups already present on the surface. For our solution-deposited molecules the protons could also originate from the solution.

The C 1s spectra, in Fig. 2, exhibit two main contributions: the small peak at high binding energy has contributions from covalently-anchored carboxylate groups at 288.7 eV and intact carboxylic acid at 289.1 eV [19]. The main peak at 284.8 eV corresponds to all remaining carbon atoms, without oxygen neighbors. In between the two peaks there is an additional small contribution from a shake-up satellite expected at 287.9 eV [12]. The broadening of the carboxylate peak towards higher binding energies for the *tetra* molecule could indicate the presence of intact carboxylic acid functional groups. However, we should bear in mind that depositing molecules from ethanolic solutions could also result in the co-deposition of carboxylic acids [20] and ethoxy groups [21] which would also broaden the C 1s XPS peak towards higher binding energy and give overlapping signals in the O 1s XPS spectra which is thus not presented.

Reference valence-band spectrum of the TiO$_2$(110) substrate in Fig. 2 (right panel) shows a broad O 2p band from 3 to 9 eV and a well-defined Ti 3d defect state at 0.8 eV [22,23]. Following adsorption of the carboxylic acid-functionalized porphyrins, the defect state decreases in intensity and new electronic states appear at 10.2, 11.0, 13.8 and 17.6 eV below the Fermi level. The intensity decrease observed in the band gap state could be due to a healing of surface defects after exposing the crystal to solution in addition to the attenuation caused by the adsorbates. The band at 11.0 eV is due to a hydroxyl 3σ state [24] and could originate from deprotonation of the carboxylic acid functional groups and/or protons from solution. The other features at 10.2, 13.8 and 17.6 eV are related to molecular states [10]. Finally, the shape of the O 2p band changes after adsorption suggesting the presence of further molecular electronic states overlapping with this band [25].

Figs. 3–5 show N K-edge NEXAFS spectra of the *mono, cis, trans* and *tetra* carboxylic acid-functionalized tetraphenylporphyrin adsorbed on TiO$_2$(110), using different incidence angles. For normal incidence, the electric field of the incoming radiation is parallel to the surface ($\alpha = 0°$, see Fig. 6) and therefore macrocycles adsorbed normal to the surface will result in maximum π* transition intensity [26]. On the contrary, for grazing incidence the electric field of the incoming radiation is normal to the surface ($\alpha = 90°$, see Fig. 6) and macrocycles adsorbed parallel to the surface will yield maximum π* transition intensity [26]. Spectra were also acquired for different azimuthal angles (ϕ) between the electric field of the incoming radiation and the [001] crystallographic direction along the bridging oxygen rows (see Fig. 6).

The NEXAFS spectra corresponding to the four molecules studied show the same electronic transitions labelled *a-g* in Figs. 3–5. This indicates that the unoccupied molecular electronic structure of the porphyrin ring is not influenced much by the number and position of the carboxylic acid functional groups. The N K-edge NEXAFS spectra show a well-defined peak *a* (398.4 eV) followed by peaks *b* (400.4 eV), *c* (401.7 eV), *d* (402.8 eV) and *e* (403.8 eV), corresponding to electronic transitions from the iminic N 1s and the aminic N 1s states to different π* molecular orbitals in the porphyrin ring [27,28]. The broad peaks *f* (~ 408 eV) and *g* (~ 417 eV) are due to transitions into different σ* molecular orbitals [27]. The precise assignment of these electronic transitions can be found elsewhere [27]. The overall shape and position of the peaks agree very well with the spectra corresponding to free base tetraphenylporphyrins adsorbed on different substrates [27,29,30]. This confirms that the molecules adsorb on TiO$_2$(110) retaining the
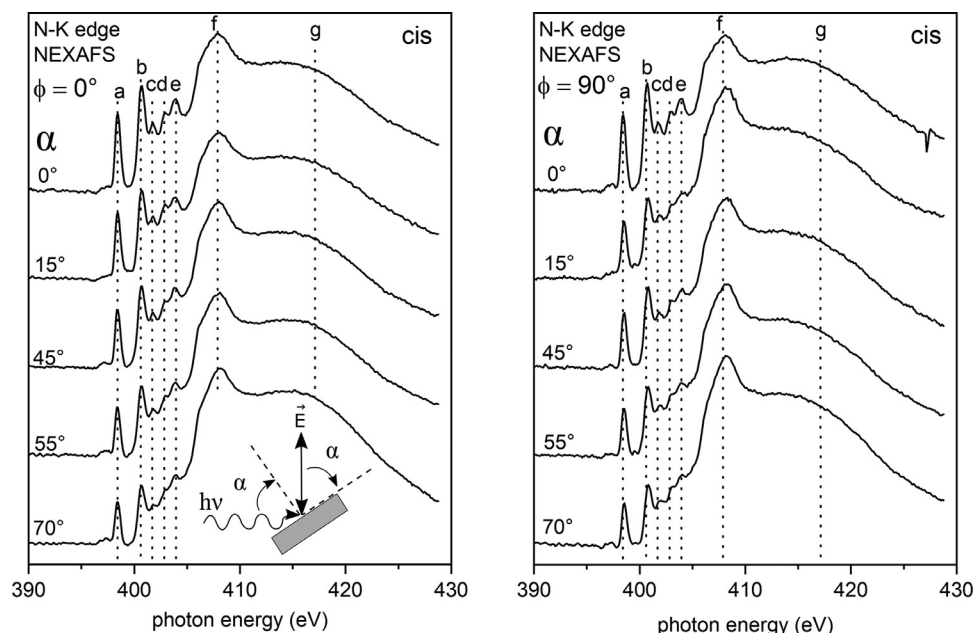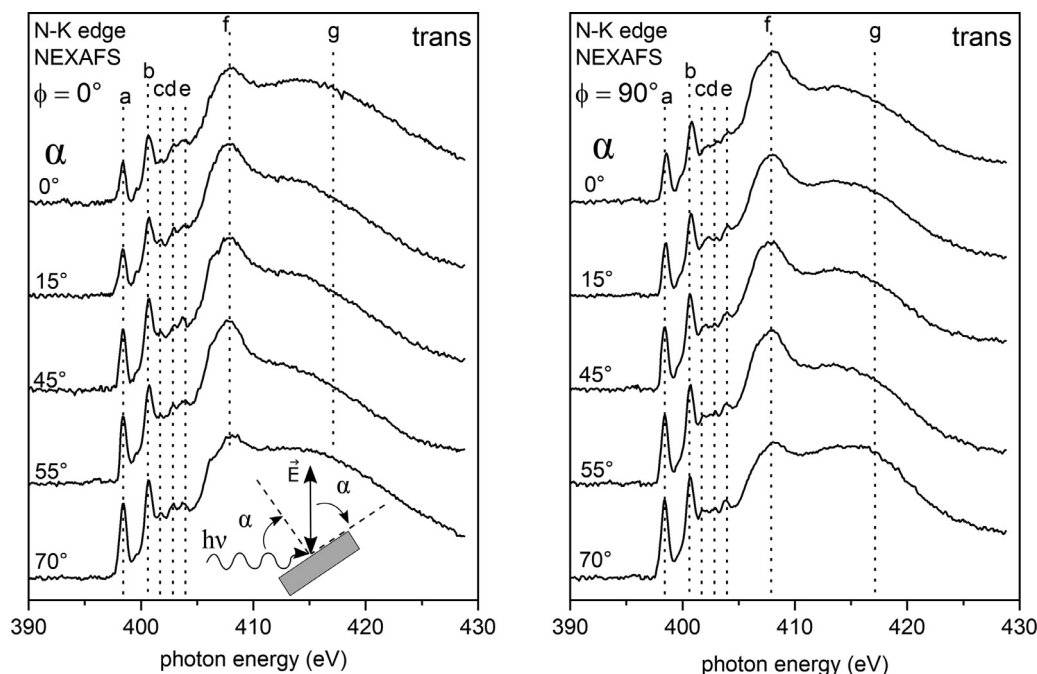
Fig. 3. N K-edge NEXAFS spectra of *cis* porphyrins adsorbed on TiO$_2$(110), measured using different incidence angles. The left panel shows spectra measured with an electric-field azimuthal angle (φ) of 0°, whereas the right panel corresponds to an azimuthal angle of 90°, relative to the oxygen rows ([001] crystallographic direction), see Fig. 6.

electronic structure of the porphyrin ring. Here we should note that, in the case of the tetra molecule, a new peak appears as a high photon energy shoulder of peak *a*. A precise assignment of this transition would require calculations of the electronic structure of *tetra* molecules on TiO$_2$(110). However, we should note that the same shoulder was observed in the N-K edge NEXAFS spectra of the same tetraphenyl porphyrin but functionalized with four phosphonic acid groups suggesting that it could be due to the molecular symmetry [31].

The spectra corresponding to *cis* molecules in Fig. 3 show that the 398.4 eV π* transition intensity decreases as the electric field angle increases. This suggests that *cis* molecules adsorb with the macrocycle standing upright. On the contrary, *trans* molecules show the opposite behavior in Fig. 4, the π* transition intensity increases with increasing the electric field angle, suggesting that *trans* molecules are flat lying. In

both cases, the spectra show no azimuthal dependence, indicating either a 45° orientation with respect to the [001] direction or that there is no preferred orientation in the plane of the monolayer. Here we should note that exposing the TiO$_2$(110) surface to air results in the adsorption of carboxylic acids (which are later displaced by the porphyrin molecules) preserving the surface crystallographic structure [20]. Furthermore, depositing multilayers of ethanol on TiO$_2$(110) and then annealing to room temperature results in a surface covered with ethoxy groups whilst maintaining the surface crystallographic structure [21]. These investigations suggest that after our surface treatment in ethanolic solutions the surface crystallographic structure should be preserved.

The N K-edge spectra of *mono* and *tetra* molecules in Fig. 5 were, unfortunately, measured only with an azimuthal angle of 0°. Strictly

Fig. 4. N K-edge NEXAFS spectra of *trans* porphyrins adsorbed on TiO$_2$(110) measured using different incidence angles. The left panel shows spectra measured with an azimuthal angle (φ) of 0° whereas the right panel corresponds to an azimuthal angle of 90° (see Fig. 6).
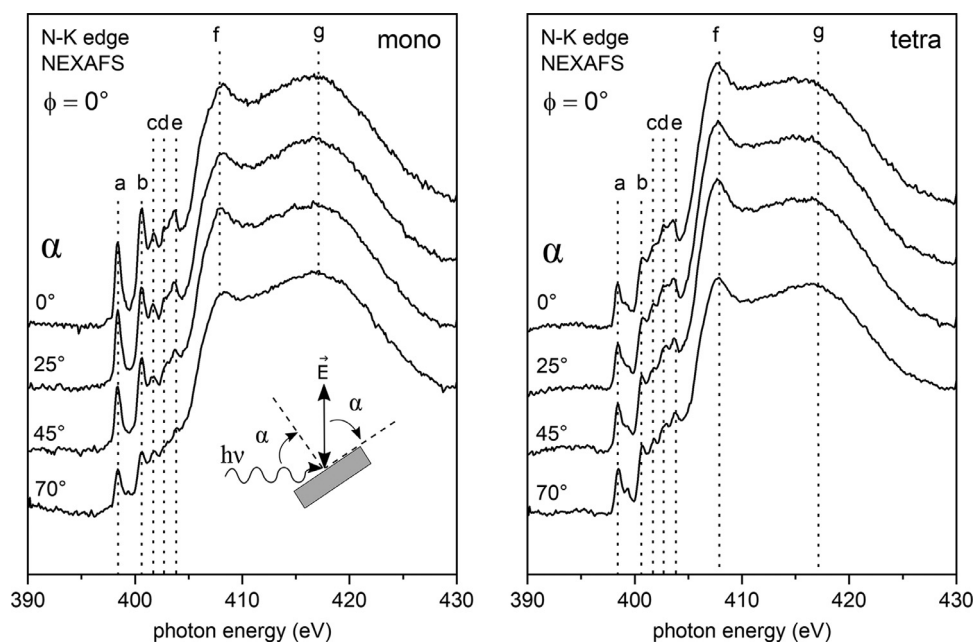
Fig. 5. N K-edge NEXAFS spectra of *mono* (left) and *tetra* (right) porphyrins adsorbed on TiO$_2$(110) measured using different incidence angles and an azimuthal angle of 0° (see Fig. 6).
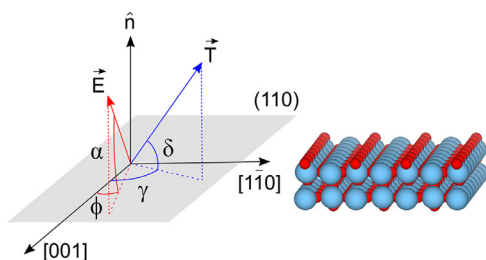

Fig. 6. The photon electric field vector ($\vec{E}$) forms a polar angle α with the surface plane and its surface component forms and azimuthal angle ϕ with the [001] crystallographic direction along the oxygen rows. The molecular transition dipole moment is a vector ($\vec{T}$) perpendicular to the aromatic ring and is characterized by a polar angle δ with respect to the surface and an azimuthal angle γ with respect to the [001] crystallographic direction.

speaking, a single azimuthal angle measurement is not sufficient to estimate the tilt angle in two-fold symmetric surfaces. However, since we saw no azimuthal dependency in the spectra corresponding to the *cis* and *trans* molecules, we assume no azimuthal dependency in the *mono* and *tetra* molecules. The π* transition intensity of the *mono* molecules decreases with increasing the electric field angle suggesting that *mono* molecules are upright standing. Finally, the spectra corresponding to *tetra* molecules show no linear dichroism suggesting an intermediate adsorption angle.

The π* transition intensity depends on the square of the scalar product of the electrical field vector $\vec{E}$ and the transition dipole moment vector $\vec{T}$ [32]. For two-fold symmetric substrates, the intensity of aromatic 1s → π* transitions is [33]:

$$I_{\pi^*}(\alpha, \delta, \phi, \gamma)$$
$$= P(\sin^2\alpha\sin^2\delta + \cos^2\alpha\cos^2\delta(\cos^2\phi\cos^2\gamma + \sin^2\phi\sin^2\gamma)) +$$
$$+ (1 - P)\cos^2\delta(\sin^2\phi\cos^2\gamma + \cos^2\phi\sin^2\gamma) \qquad (1)$$

where P is the degree of polarization ($P = 1$ for perfectly linearly polarized light), α is the angle between the electrical field vector $\vec{E}$ and the surface and ϕ is the azimuthal rotation of $\vec{E}$ in the surface plane. The orientation of the molecule is characterized by the angle δ between

the transition dipole moment $\vec{T}$ and the surface, and the angle γ, which corresponds to the azimuthal rotation of the transition dipole moment in the surface plane. For two-fold symmetry substrates, one expects four adsorption domains, due to the substrate mirror planes perpendicular to the surface along the [001] and the [1$\bar{1}$0] azimuthal directions. Given that NEXAFS spectroscopy averages over the four domains, the observed intensity is equal to the sum of the intensities corresponding to (δ, γ), (δ, -γ), (-δ,γ) and (-δ,-γ).

Fig. 7 shows the normalized intensity of the 398.4 eV π* transition as a function of the electric field angle α for the *cis-, trans-, mono-* and *tetra*-functionalized tetraphenylporphyrin molecules adsorbed on TiO$_2$(110). As discussed above, the intensities of *cis* and *mono* decrease with increasing the electric field angle, the intensities of *trans* increases and the intensity of *tetra* remains constant. In order to estimate adsorption angles, the data in Fig. 7 was fitted with Eq. (1) considering the four mirror domains discussed above and simultaneously fitting both polar (δ) and azimuthal (γ) angles. This resulted in polar angles of δ = 25° (molecular tilt angle of 65° from the surface) for *cis* molecules and δ = 45° for *trans* molecules and azimuthal angles of 45° for both molecules. Note that an azimuthal angle of 45° is also compatible with random azimuthal adsorption angles. Also, we should note that flat-lying tetraphenylporphyrin molecules could give an apparent NEXAFS tilt angle of ~35° to ~45°, because the macrocycle ring could distorted with a saddle-shape or inverted geometry [34]. Thus, the NEXAFS data suggests that *cis* molecules adsorb with the macrocycle tilted away from the surface and *trans* molecules adsorb with the macrocycle closer to the surface.

As mentioned above, the spectra corresponding to *mono* and *tetra* molecules were only measured for one azimuthal angle ϕ = 0°, which is not sufficient to fit the data unambiguously in two-fold symmetric surfaces. Nevertheless, because we observe no azimuthal dependency for the *cis* and *trans* molecules, we assume no azimuthal dependence for the *mono* and *tetra* molecules. That is, we assume an azimuthal adsorption angle of 45° (or random azimuthal orientation, as the two situations cannot be distinguished). This results in a macrocycle tilted 66° with respect to the surface for *mono* molecules. The tilt angle estimated for *mono* molecules is essentially the same as the value of 65° estimated for *cis* molecules. For *tetra* molecules, the π* transition intensity is independent of the electric field angle, which indicates that either the
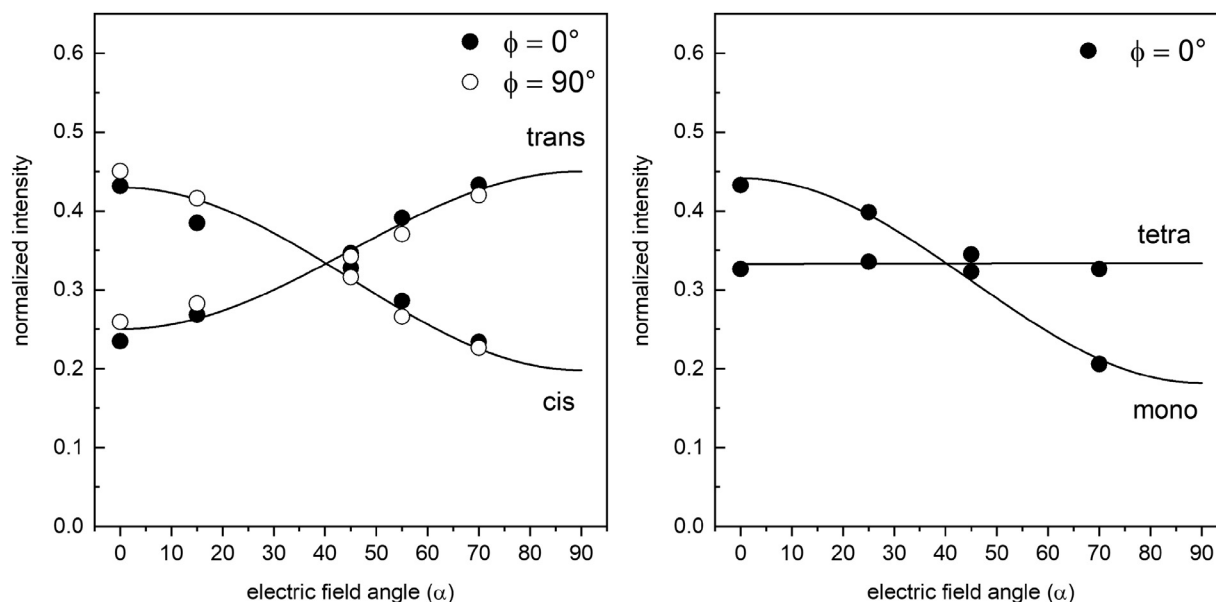
Fig. 7. Normalized π* transition intensity as a function of the incoming radiation electric field angle for the *cis, trans, mono* and *tetra* functionalized tetra-phenylporphyrins adsorbed on TiO₂(110). Full lines correspond to fittings using Eq. (1) taking into account the four mirror domains expected in two-fold symmetry substrates.

molecules are randomly oriented, all adsorbed with an angle of 54.7°, or a combination of upright standing and flat-lying. Given that 2 –COOH groups in *cis* positions result in tilted molecules and that 2 –COOH groups in *trans* positions results in approximately flat-lying molecules, it is tempting to assume that *tetra* molecules could arbitrarily behave like *cis* or *trans* molecules which could result in a layer composed of a mixture of upright standing and flat lying molecules. Notably, our spectroscopic data does not yield a complete atomic description of porphyrin binding to the surface, for this density functional theory calculations would need to be undertaken.

4. Conclusions

Adsorption of carboxylic acid-functionalized tetraphenylporphyrin molecules on TiO₂(110) surfaces at the solid/liquid interface results in partial protonation of the iminic nitrogen atoms at the macrocycle. The spectroscopic signature of the molecules indicates that molecules retain their electronic structure after adsorption. The number and position of carboxylic acid functional groups control the molecular adsorption geometry. Porphyrins with one –COOH functional group or two in a *cis* configuration adsorb with the macrocycle tilted away from the surface plane. On the contrary, two –COOH functional groups in a *trans* configuration result in more flat-lying molecules. Finally, molecules with four –COOH functional groups adsorb with an intermediate average adsorption angle.

Acknowledgements

References

[1] J.V. Barth, Molecular architectonic on metal surfaces, Annu. Rev. Phys. Chem. 58 (2007) 375–407, https://doi.org/10.1146/annurev.physchem.56.092503.141259.

[2] W. Auwärter, D. Écija, F. Klappenberger, J.V. Barth, Porphyrins at interfaces, Nat. Chem. 7 (2015) 105–120, https://doi.org/10.1038/nchem.2159.

[3] J.A.A.W. Elemans, R. van Hameren, R.J.M. Nolte, A.E. Rowan, Molecular materials by self-assembly of porphyrins, phthalocyanines, and perylenes, Adv. Mater. 18 (2006) 1251–1266, https://doi.org/10.1002/adma.200502498.

[4] D. Filippini, A. Alimelli, C. Di Natale, R. Paolesse, A. D'Amico, I. Lundström, Chemical sensing with familiar devices, Angew. Chemie Int. Ed. 45 (2006) 3800–3803, https://doi.org/10.1002/anie.200600050.

[5] J. Shen, R. Kortlever, R. Kas, Y.Y. Birdja, O. Diaz-Morales, Y. Kwon, I. Ledezma-Yanez, K.J.P. Schouten, G. Mul, M.T.M. Koper, Electrocatalytic reduction of carbon dioxide to carbon monoxide and methane at an immobilized cobalt protoporphyrin, Nat. Commun. 6 (2015) 8177, https://doi.org/10.1038/ncomms9177.

[6] M.A. Baldo, D.F. O'Brien, Y. You, A. Shoustikov, S. Sibley, M.E. Thompson, S.R. Forrest, Highly efficient phosphorescent emission from organic electro-luminescent devices, Nature 395 (1998) 151–154, https://doi.org/10.1038/25954.

[7] A. Yella, H.-W. Lee, H.N. Tsao, C. Yi, A.K. Chandiran, M.K. Nazeeruddin, E.W.-G. Diau, C.-Y. Yeh, S.M. Zakeeruddin, M. Gratzel, Porphyrin-sensitized solar cells with cobalt (II/III)-based redox electrolyte exceed 12 percent efficiency, Science 334 (2011) 629–634, https://doi.org/10.1126/science.1209688.

[8] A. Fakharuddin, R. Jose, T.M. Brown, F. Fabregat-Santiago, J. Bisquert, A perspective on the production of dye-sensitized solar modules, Energy Environ. Sci. 7 (2014) 3952–3981, https://doi.org/10.1039/C4EE01724B.

[9] J. Köbl, T. Wang, C. Wang, M. Drost, F. Tu, Q. Xu, H. Ju, D. Wechsler, M. Franke, H. Pan, H. Marbach, H.-P. Steinrück, J. Zhu, O. Lytken, Hungry Porphyrins, Protonation and self-metalation of tetraphenylporphyrin on TiO₂ (110) - 1 × 1, ChemistrySelect 1 (2016) 6103–6105, https://doi.org/10.1002/slct.201601398.

[10] G. Lovat, D. Forrer, M. Abadia, M. Dominguez, M. Casarin, C. Rogero, A. Vittadini, L. Floreano, Hydrogen capture by porphyrins at the TiO₂ (110) surface, Phys. Chem. Chem. Phys. 17 (2015) 30119–30124, https://doi.org/10.1039/C5CP05437K.

[11] G. Lovat, D. Forrer, M. Abadia, M. Dominguez, M. Casarin, C. Rogero, A. Vittadini, L. Floreano, On-Surface synthesis of a pure and long-range-ordered titanium(iv)-porphyrin contact layer on titanium dioxide, J. Phys. Chem. C 121 (2017) 13738–13746, https://doi.org/10.1021/acs.jpcc.7b03157.

[12] D. Wechsler, C.C. Fernández, H.-P. Steinrück, O. Lytken, F.J. Williams, Covalent anchoring and interfacial reactions of adsorbed porphyrins on rutile TiO₂ (110), J. Phys. Chem. C 122 (2018) 4480–4487, https://doi.org/10.1021/acs.jpcc.7b12717.

[13] K. Werner, S. Mohr, M. Schwarz, T. Xu, M. Amende, T. Döpper, A. Görling, J. Libuda, Functionalized porphyrins on an atomically defined oxide surface: anchoring and coverage-dependent reorientation of MCTPP on CO₃ O₄ (111), J. Phys. Chem. Lett. 7 (2016) 555–560, https://doi.org/10.1021/acs.jpclett.5b02784.

[14] F. Kollhoff, J. Schneider, G. Li, S. Barkaoui, W. Shen, T. Berger, O. Diwald, J. Libuda, Anchoring of carboxyl-functionalized porphyrins on MgO, TiO₂, and CO₃ O₄ nanoparticles, Phys. Chem. Chem. Phys. (2018), https://doi.org/10.1039/C8CP04873H.

[15] A. Rienzo, L.C. Mayor, G. Magnano, C.J. Satterley, E. Ataman, J. Schnadt, K. Schulte, J.N. O'Shea, X-ray absorption and photoemission spectroscopy of zinc protoporphyrin adsorbed on rutile TiO₂(110) prepared by in situ electrospray deposition, J. Chem. Phys. 132 (2010) 084703, , https://doi.org/10.1063/1.3336747.

[16] R. Jöhr, A. Hinaut, R. Pawlak, Ł. Zajac, P. Olszowski, B. Such, T. Glatzel, J. Zhang, M. Muntwiler, J.J. Bergkamp, L.-M. Mateo, S. Decurtins, S.-X. Liu, E. Meyer, Thermally induced anchoring of a zinc-carboxyphenylporphyrin on rutile TiO₂(110), J. Chem. Phys. (2017) 146, https://doi.org/10.1063/1.4982936.

[17] R. Jöhr, A. Hinaut, R. Pawlak, A. Sadeghi, S. Saha, S. Goedecker, B. Such, M. Szymonski, E. Meyer, T. Glatzel, Characterization of individual molecular adsorption geometries by atomic force microscopy: Cu-TCPP on rutile TiO$_2$(110), J. Chem. Phys (2015) 143, https://doi.org/10.1063/1.4929608.

[18] D.H. Karweik, N. Winograd, Nitrogen charge distributions in free-base porphyrins, metalloporphyrins, and their reduced analogs observed by x-ray photoelectron spectroscopy, Inorg. Chem. 15 (1976) 2336–2342, https://doi.org/10.1021/ic50164a003.

[19] M. Franke, F. Marchini, L. Zhang, Q. Tariq, N. Tsud, M. Vorokhta, M. Vondráček, K. Prince, M. Röckert, F.J. Williams, H.-P. Steinrück, O. Lytken, Temperature-dependent reactions of phthalic acid on Ag(100), J. Phys. Chem. C. 119 (2015) 23580–23585, https://doi.org/10.1021/acs.jpcc.5b07858.

[20] J. Balajka, M.A. Hines, W.J.I. DeBenedetti, M. Komora, J. Pavelec, M. Schmid, U. Diebold, High-affinity adsorption leads to molecularly ordered interfaces on TiO$_2$ in air and solution, Science 361 (2018) 786–789, https://doi.org/10.1126/science.aat6752.

[21] C.P. León, K. Sagisaka, D. Fujita, L. Han, Ethanol adsorption on rutile TiO$_2$(110), RSC Adv. 4 (2014) 8550, https://doi.org/10.1039/c3ra47369d.

[22] C.M. Yim, C.L. Pang, G. Thornton, Oxygen vacancy origin of the surface band-gap state of TiO$_2$(110), Phys. Rev. Lett. 104 (2010) 036806, , https://doi.org/10.1103/PhysRevLett.104.036806.

[23] K. Mitsuhara, H. Okumura, A. Visikovskiy, M. Takizawa, Y. Kido, The source of the Ti$_3$ d defect state in the band gap of rutile titania (110) surfaces, J. Chem. Phys. 136 (2012) 124707, , https://doi.org/10.1063/1.3697866.

[24] W. Zhang, L. Liu, L. Wan, L. Liu, L. Cao, F. Xu, J. Zhao, Z. Wu, Electronic structures of bare and terephthalic acid adsorbed TiO$_2$ (110)-(1 × 2) reconstructed surfaces: origin and reactivity of the band gap states, Phys. Chem. Chem. Phys. 17 (2015) 20144–20153, https://doi.org/10.1039/C5CP01298H.

[25] L. Giovanelli, H.-L. Lee, C. Lacaze-Dufaure, M. Koudia, S. Clair, Y.-P. Lin, Y. Ksari, J.-M. Themlin, M. Abel, A.A. Cafolla, Electronic structure of tetra(4-aminophenyl) porphyrin studied by photoemission, UV–Vis spectroscopy and density functional theory, J. Electron Spectros. Relat. Phenomena. 218 (2017) 40–45, https://doi.org/10.1016/j.elspec.2017.05.005.

[26] J. Stöhr, D.A. Outka, Determination of molecular orientations on surfaces from the angular dependence of near-edge x-ray-absorption fine-structure spectra, Phys. Rev. B. 36 (1987) 7891–7905, https://doi.org/10.1103/PhysRevB.36.7891.

[27] K. Diller, F. Klappenberger, M. Marschall, K. Hermann, A. Nefedov, C. Wöll, J.V. Barth, Self-metalation of 2H-tetraphenylporphyrin on Cu(111): an x-ray spectroscopy study, J. Chem. Phys. 136 (2012) 014705, , https://doi.org/10.1063/1.3674165.

[28] G. Di Santo, C. Castellarin-Cudia, M. Fanetti, B. Taleatu, P. Borghetti, L. Sangaletti, L. Floreano, E. Magnano, F. Bondino, A. Goldoni, Conformational adaptation and electronic structure of 2H-tetraphenylporphyrin on Ag(111) during Fe metalation, J. Phys. Chem. C. 115 (2011) 4155–4162, https://doi.org/10.1021/jp111151n.

[29] N. Schmidt, R. Fink, W. Hieringer, Assignment of near-edge x-ray absorption fine structure spectra of metalloporphyrins by means of time-dependent density-functional calculations, J. Chem. Phys. 133 (2010) 054703, , https://doi.org/10.1063/1.3435349.

[30] M. Chen, X. Feng, L. Zhang, H. Ju, Q. Xu, J. Zhu, J.M. Gottfried, K. Ibrahim, H. Qian, J. Wang, Direct synthesis of nickel(II) tetraphenylporphyrin and its interaction with a Au(111) surface: a comprehensive study, J. Phys. Chem. C. 114 (2010) 9908–9916, https://doi.org/10.1021/jp102031m.

[31] C.C. Fernández, D. Wechsler, T.C.R. Rocha, H.-P. Steinrück, O. Lytken, F.J. Williams, Adsorption of phosphonic-acid-functionalized porphyrin molecules on TiO$_2$ (110), J. Phys. Chem. C. 123 (2019) 10974–10980, https://doi.org/10.1021/acs.jpcc.9b01019.

[32] J. Stöhr, NEXAFS Spectroscopy, Springer Berlin Heidelberg, Berlin, Heidelberg, 1992, https://doi.org/10.1007/978-3-662-02853-7.

[33] J. Stöhr, M.G. Samant, Liquid crystal alignment by rubbed polymer surfaces: a microscopic bond orientation model, J. Electron Spectros. Relat. Phenomena. 98–99 (1999) 189–207, https://doi.org/10.1016/S0368-2048(98)00286-2.

[34] D. Wechsler, M. Franke, Q. Tariq, L. Zhang, T.-L. Lee, P.K. Thakur, N. Tsud, S. Bercha, K.C. Prince, H.-P. Steinrück, O. Lytken, Adsorption structure of cobalt tetraphenylporphyrin on Ag(100), J. Phys. Chem. C. 121 (2017) 5667–5674, https://doi.org/10.1021/acs.jpcc.7b00518.